CHEMISTRY JOURNAL OF MOLDOVA. General, Industrial and Ecological Chemistry. 2024, 19(2), 7-15
ISSN (p) 1857-1727 ISSN (e) 2345-1688
http://cjm.ichem.md
https://doi.org/10.19261/cjm.2024.1196

THE POTENTIAL OF RICE HUSK WASTE TO SYNTHESISE ZINC OXIDE NANOPARTICLES AND ASSESSMENT TO THE ANTIBACTERIAL ACTIVITIES

Nurfitrah Amran [a], Siti NurSyazwani Maadon [a], Yamin Yasin [b], Nik Rozlin Nik Masdek [c], Mohd Rafii Yusop [d], Nor Hazlina Mat Sa'at [e], Nor Monica Ahmad [b], Nor'Aishah Hasan [a*]

[a]*School of Biology, Faculty of Applied Sciences, MARA University of Technology, Cawangan Negeri Sembilan, Kampus Kuala Pilah, 72000 Kuala Pilah, Malaysia*
[b]*School of Chemistry and Environment, Faculty of Applied Sciences, MARA University of Technology, Cawangan Negeri Sembilan, Kampus Kuala Pilah, 72000 Kuala Pilah, Malaysia*
[c]*School of Mechanical Engineering, College of Engineering, MARA University of Technology, 40450 Shah Alam, Selangor, Malaysia*
[d]*Institute of Tropical Agriculture and Food Security, University of Putra Malaysia (UPM), Serdang, Selangor, Malaysia*
[e]*Horticulture Research Centre, Malaysian Agricultural Research and Development Institute, Persiaran-UPM 43400 Serdang, Selangor, Malaysia*
[*]*e-mail: aishahnh@uitm.edu.my*

Abstract. In the past decade, open-air burning of rice husks has negatively impacted the environment and human health, particularly in developing and underdeveloped nations. Consequently, the present study established a sustainable and environmentally friendly method of manufacturing zinc oxide nanoparticles (ZnO NPs) from *Oryza sativa* rice husks using different concentrations of the precursor. The ZnO NPs obtained were analysed with an ultraviolet-visible (UV-Vis) spectrophotometer, which revealed a characteristic ZnO NPs band at 410 nm. Based on Debye-Scherrer's equation, the ZnO NPs crystallites had a mean size of 20 nm. The Fourier-transform infrared (FTIR) spectra of the ZnO NPs were determined within the 400 to 4000 cm^{-1} range. The peak at 487 cm^{-1} indicated that a Zn-O bond was formed. A developed material further evaluated the antibacterial effectiveness of ZnO NPs against four harmful bacteria, demonstrating a moderate level of effectiveness. The findings indicated that all the tested bacteria exhibited heightened susceptibility to ZnO NPs at a higher concentration of 250 µg/mL.

Keywords: rice husk waste, *Oryza sativa*, zinc oxide, nanoparticles, antibacterial activity.

Received: 16 July 2024/ Revised final: 11 October 2024/ Accepted: 14 October 2024

Introduction

The introduction and development of nanotechnology offered numerous possible accomplishments through material manipulation. Nanotechnology has also altered the worldwide paradigm due to its applications in various areas [1], and advancements have resulted in smart materials with unique nanoparticle (NP) properties. The minute size of NP, between 1 and 100 nm, and its significant surface-to-volume ratio have enabled it to be employed in numerous fields, including medicine [2], cosmetics [3], photocatalytic [4], electronics [5], and agriculture [6].

Utilising plant extracts from various plant species to biosynthesise nanoparticles (NPs) has been widely explored, encompassing numerous metals, such as copper [7], gold [8], and silver [9]. Zinc oxide (ZnO) is emerging as a particularly compelling inorganic oxide and gaining the interest of researchers due to its versatility and wide-ranging applications [10,11]. ZnO NPs are widely employed in different industries, including drug delivery, solar cells, medicals, photocatalytic degradation, and personal care products, such as sunscreen and cosmetics, as they are non-toxic, biocompatible, and cost-effective [11-13]. ZnO NPs could be fabricated through a plethora of physicochemical pathways, including sol-gel, co-precipitation, laser vaporisation, microemulsion, and ball milling [14-17].

Nevertheless, conventional nanomaterial synthesising techniques are costly and require toxic and harmful reagents, organic solvents, and non-biodegradable stabilising agents [18,19]. Physicochemical processes of manufacturing

ZnO NPs also involve very complex procedures and costly equipment and consume considerable time and energy [20].

A "green chemistry" approach is necessary in manufacturing NPs. The technique employs safe, non-toxic, and environmentally sustainable methodologies that could be utilised in open areas. Biosynthetic NPs are more water soluble biocompatible and less hazardous [21]. Organic materials are crucial in producing green NPs, and the methods are regarded as valuable alternatives to the chemical approaches [22].

Numerous reports on ZnO NPs biosynthesis approaches are available. For instance, Saka, A. *et al.,* produced ZnO NPs with *Apocynaceae, Carissa spinarum L.* (Hagamsa) leaf extract. The study obtained relatively small (45.76 nm) cauliflower-shaped NPs, which was an excellent antibacterial agent [23]. In another study, Abdelbaky, A.S. *et al.,* employed apple geranium (*Pelargonium odoratissimum)* leaf extract. The numerous phytoconstituents in the leaf extract acted as capping agents, resulting in ZnO NPs with excellent features. The NPs reported in the literature were 76 nm and spherical and hexagonal [10]. Nonetheless, a smaller (34.23 nm) spherical ZnO NPs was yielded when *Aquilegia pubiflora* (Himalayan Columbine) was utilised as reported by Jan, H. *et al.* [24].

Reports on synthesising ZnO NPs with agricultural wastes are scarce. Rice husk (RH) is a promising material in NPs production, including silica and silica oxide NPs [25,26]. Open-air burning of RH, a waste product, has impacted the environment and human health, especially in developing and underdeveloped countries [27]. Moreover, processing and transporting RH are laborious due to its low density and low commercial value, leading to disposal issues and significant environmental harm [28].

The present study was the first to employ bio-assisted ZnO NPs production through a simple and eco-friendly approach utilising *Oryza sativa* RH. The green ZnO NPs were extensively examined with various characterisation techniques, including ultraviolet-visible (UV-Vis) spectroscopy, X-ray diffraction (XRD), transmission electron microscopy (TEM), Fourier-transform infrared (FTIR), and scanning electron microscopy-energy dispersive X-ray (SEM-EDX). The NPs obtained in this study were also employed as an antibacterial agent against *Escherichia coli*, *Bacillus subtilis*, *Klebsiella pneumoniae*, and *Staphylococcus aureus*.

Experimental

Materials

The current study employed zinc sulphate heptahydrate (Duchefa Biochemie, Netherland), hydrochloric acid (HCl) (RCI Labscan, Thailand), sodium hydroxide (NaOH) (R&M Chemicals, Malaysia), ethanol (Fisher Scientific, United Kingdom), Mueller-Hinton agar (Oxoid, United Kingdom), nutrient broth (Merck Millipore, Germany), and deionised water without purification.

Preparing the rice husk ash

In this study, the RH ash (RHA) was prepared according to the guideline reported by Nguyen, H.X. *et al.*, with slight modifications [28]. Firstly, the RH was washed thoroughly under running water to remove heavy impurities, such as sand, dust, and other contaminants that might be present. Subsequently, the material was air-dried for 30 min before it was soaked in 2 M HCl for 1 h to remove small quantities of minerals before extracting silica from the RH. The RH was oven-dried for 24 h at 80°C before being burned in a furnace for 5 h at 700°C to obtain RHA.

Synthesising the ZnO NPs with the RH solution

The ZnO NPs in the present study were produced according to the procedures outlined by Saka, A. *et al.* [23], Jayachandran, A.T.R.A. *et al.* [29], and Balogun, S.W. *et al.* [5] with modifications. The plant extract was substituted with sodium silicate derived from RHA as a capping agent in this altered method. This substitution was made to enhance the stability and control the growth of the ZnO NPs, thereby preventing agglomeration and improving their dispersion. First, 1.0 g of the RHA was mixed with 200 mL of 2 M NaOH solution under agitation at room temperature to obtain sodium silicate. After 1 h of agitation, zinc sulphate heptahydrate and 200 mL of 2 M HCl were added to the sodium silicate solution to achieve pH 7, yielding a mixture containing Zn^{2+} and silicate ion (SiO_4^-).

Varying the concentration of zinc sulphate heptahydrate masses (0.4 M, 0.8 M, 1.2 M, 1.6 M and 2.0 M) were boiled with 200 mL of a solution containing silicon dioxide (SiO_2) with a stirrer-heater at 50°C to observe the effects of precursor concentration. Subsequently, the mixture was boiled for 5 h until a white precipitate formed before centrifuging the precipitate at 3000 rpm for 2 min. The precipitate was washed twice with ethanol and distilled water to remove dirt and impurities. The greyish precipitate was then collected and oven-dried for 24 h at 80°C.

The dried samples were ground and placed in a furnace to calcine for 3 h at 500°C before they were ground again. The specimens were weighed and stored as NPs (Figure S1 in supplementary information).

Characterisations of the prepared ZnO NPs

The optical properties of ZnO NPs were examined using a UV-Vis spectrophotometer (T80+, PG Instruments) over the wavelength range of 300-700 nm. The crystalline structure and phase purity of ZnO NPs were determined using a Rigaku diffractometer. The morphology and elemental composition of ZnO NPs were analysed using a Hitachi TM3030 PLUS SEM equipped with EDX analysis. Detailed insights into the internal structure and crystallinity of ZnO NPs were obtained using a Talos L120C TEM. The functional groups and bonding characteristics of ZnO NPs were investigated using FTIR (Perkin Elmer) in the range of 4000−400 cm^{-1}.

The ZnO NPs antibacterial activities

The antibacterial effectiveness of the ZnO NPs manufactured in this study against *Bacillus subtilis* (*B. subtilis*), *Staphylococcus aureus* (*S. aureus*), *Escherichia coli* (*E. coli*), and *Klebsiella pneumoniae* (*K. pneumoniae*) was assessed through the disc diffusion technique. The procedures were adapted from the guidelines reported by Ali, D. *et al.* [30], Karthik, M. *et al.* [31], and Kamarajan, G. *et al.* [32]. First, blank discs were soaked with 50, 100, 150, 200, and 250 µg/mL of the biosynthesised ZnO NPs. Agar plates containing the bacterial strains and carefully placed discs soaked with the ZnO NPs were incubated for 24 h at 37°C. The present study employed Ciprofloxacin and distilled water as the positive and negative controls, respectively. The inhibition zone diameter observed on each plate was determined and all experiments were performed in triplicates.

Results and discussion

This section aims to characterise ZnO NPs utilising UV-Vis spectroscopy, XRD, and FTIR. Additionally, a detailed morphological analysis and the shape of the NPs were conducted using TEM and SEM-EDX.

UV-Vis analysis

UV-Vis spectrophotometry was employed to establish the optical properties of the ZnO NPs manufactured in the current study. The NPs were synthesised through a green methodology exploiting *Oryza sativa* rice husks as the reducing and capping agent. The maximum absorbance peak observed at 398 nm confirmed the formation of ZnO NPs (Figure 1). The finding was consistent with the study by Sakthivel, S. *et al.*, where the ZnO NPs were prepared with *Citrus limon* (L.) seed aqueous extract [33]. Iqbal, J. *et al.*, also reported similar results with synthesised ZnO NPs utilising *Elaeagnus angustifolia* L. leaf extract [34].

The ZnO NPs synthesised with 1.2 M of zinc sulphate heptahydrate precursor recorded the highest absorbance band, hence the optimal precursor mass. Although higher concentrations of precursors (1.6 M and 2.0 M) were employed, the NPs documented decreased absorbance. The phenomenon might be due to the significant amounts of plant biomolecules that were still in the NPs, which stabilised the NPs by preventing new crystal developments as observed by Demissie, M.G. *et al.*, which procured ZnO NPs with *Lippia adoensis* (Koseret) leaf extract [1].

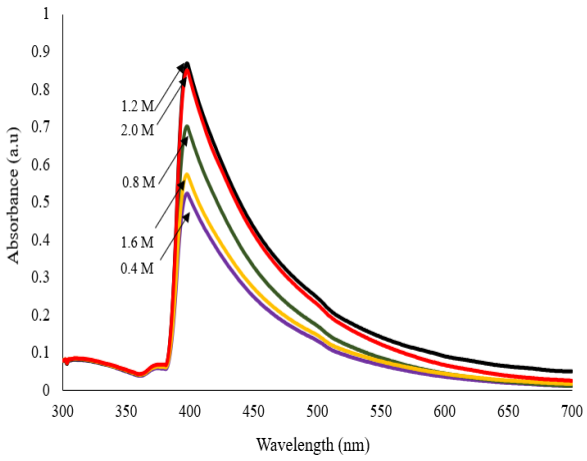

Figure 1. UV-Vis spectra of ZnO NPs in various concentrations of precursor.

XRD analysis

The XRD pattern of the ZnO NPs procured in this study is illustrated in Figure 2. The 2θ peaks were observed at 31.90°, 34.57°, 36.37°, 47.62°, 56.78°, 62.96°, 66.44°, 68.00°, 69.14°, 72.73°, 77.16°, and 81.57°, corresponding to (100), (002), (101), (102), (110), (103), (200), (112), (201), (004), (202), and (104) lattice plane values, respectively. The results were in accordance with the data reported by Sundrarajan, M. *et al.*, which produced ZnO NPs with *Pongamia pinnata* plant extract and calcined at 350°C [35]. Jayappa, M.D. *et al.*, also recorded similar findings, documenting outstanding XRD diffraction peaks of ZnO NPs manufactured with the leaf, stem and in-vitro-grown callus of *Mussaenda frondosa* (L.) [36].

In this study, the crystallite sizes of the NPs developed by varying concentrations of precursor were determined according to Debye-Scherrer's

equation. The crystallites size of ZnO NPs were determined as 19.88, 20.38, and 20.02 nm when 0.4, 0.8, and 1.2 M of precursor were employed, respectively. The crystallites procured in the current study were smaller than the NPs produced by Velsankar, K. *et al.* (29 nm) [19] and Iqbal, J. *et al.* (26 nm) [34].

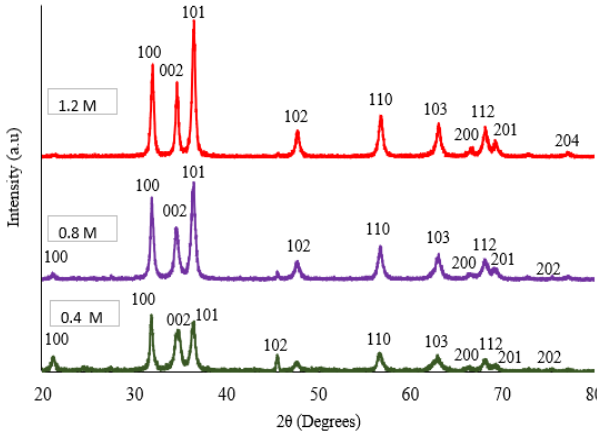

Figure 2. XRD pattern of ZnO NPs.

TEM analysis

The TEM analysis (Figure 3) conducted in the present study verified ZnO NPs formation. Based on the results, the pure green ZnO NPs exhibited rod and worm-like shapes. The aggregation observed in this study might be attributed to the high surface energy of the ZnO NPs and potential densification due to the narrow space between the particles [36]. Ansari, A. *et al.*, documented similar findings of predominantly rod-shaped NPs [37]. Gangwar, J. *et al.*, also demonstrated that most ZnO NPs produced in their ZnO NPs mediated by *Strobilanthes hamiltoniana* were rods with minimal thickness variation [38]. According to a 50 nm scale, the average particle size of 80 randomly selected ZnO NPs is 17.84 ± 3.96 nm, as depicted in Figure 3*(c)* which displays the histogram of size distribution. The findings were analysed using ImageJ software are in line with the particle sizes reported by the Scherrer's formula.

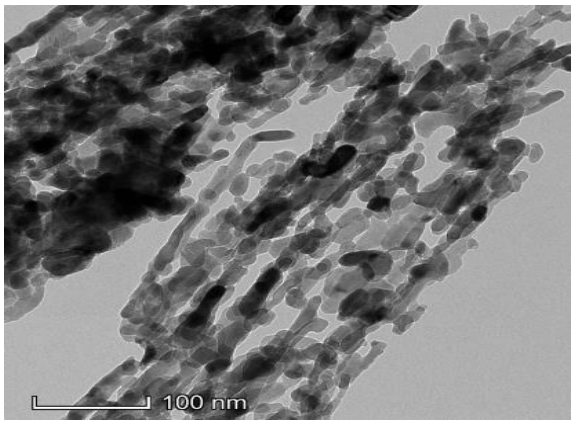

(a)

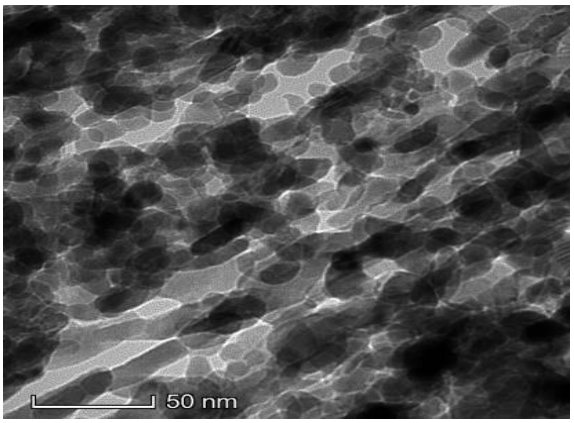

(b)

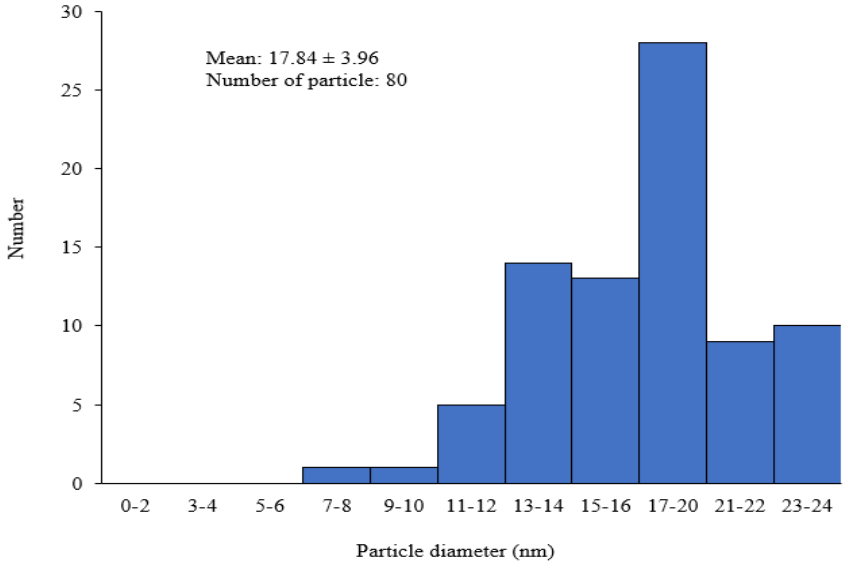

(c)

Figure 3. TEM of ZnO NPs at 100 nm magnification *(a)*, 50 nm magnification *(b)* and histogram plot*(c)*.

FTIR analysis

The band at 3431 cm^{-1} documented by the ZnO NPs manufactured in the present study represented the hydroxyl (O-H) group vibration from an intra-molecular hydrogen bond stretching. The vibrations were due to the moisture absorbed from the atmosphere. Demissie, M.G. *et al.* prepared ZnO NPs using *Lippia adoensis* (Koseret) leaf extract and noted broad peaks at approximately 3414 and 3442 cm^{-1}, suggesting similar considerable energy regions due to O-H stretching [1].

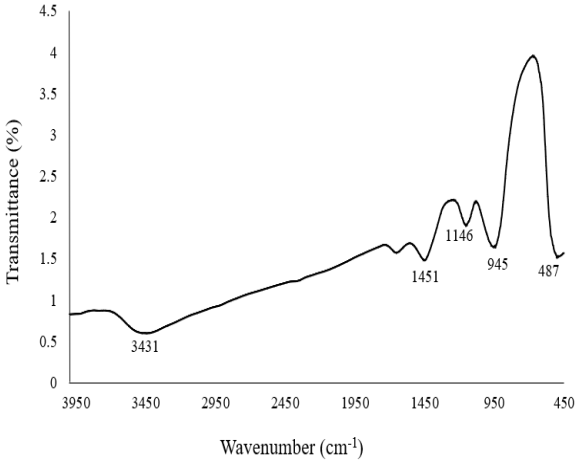

Figure 4. FTIR of ZnO NPs.

The band at 1451 cm^{-1} corresponded to the C=C stretching vibration of alkene groups in biomolecules, which might be present on the free surfaces of the NPs. Iqbal, J. *et al.*, also reported a band at 1458 cm^{-1} related to C=C stretching. On the other hand, C-O-C absorption of the ZnO NPs procured in this study was noted at 1146 cm^{-1} [34]. A band stretch at 1161 cm^{-1} was also attributed to C-O-C functional groups in the study conducted by Al Awadh, A.A. *et al.* [18]. The ZnO NPs bands observed at 994 and 487 cm^{-1} were associated with metal-oxygen, substantiating the characteristic Zn-O bonds that exist in the ZnO NPs synthesised. The observations were in agreement with the findings of Velsankar, K. *et al.*, where bands with vibrations stretching under 1000 cm^{-1} were most likely due to metal-oxygen bonding (Figure 4) [19].

SEM-EDX analysis

Figure 5 demonstrates the shapes and surface morphologies of the ZnO NPs biosynthesised in the current study. The morphology structural analysis suggested the ZnO NPs have varying and irregular quadrilateral crystals. The results were in accordance with the data reported by Devi, K. *et al.*, which documented nano flakes-like structures that agglomerated randomly ZnO NPs [39]. Similarly, Suhel, A. *et al.* recorded outstanding SEM images of irregular-shaped ZnO NPs [40].

The EDX findings documented in the present study exhibited pronounced zinc (54.4%) and oxygen (19.0%) signals, confirming the presence of zinc oxide (Figure 5*(e)*). Jayachandran, A.T.R.A. *et al.*, also noted similar elevated energy areas due to ZnO NPs, recording 78.32% and 12.78% Zn and oxygen, respectively [29]. In another study, the EDX results reported by Shaghaghi, Z. *et al.* verified the presence of Zn and O elements at 39.87% and 30.63% respective weight percentages [41]. However, the zinc content in this study is lower than the 73.29% reported by Pekdemir, S. *et al*., where *Eupatorium cannabinum* L. was employed as both a reducing and capping agent in the synthesis of ZnO NPs [42].

Antibacterial evaluation

The ZnO NPs procured in the current study exhibited antibacterial activities against *S. aureus*, *B. subtilis*, *E. coli*, and *K. pneumoniae* (Figure 6). Nevertheless, Ciprofloxacin recorded the largest inhibition zone, indicating the highest resistance as the positive control. Conversely, the negative control, distilled water, did not demonstrate any inhibition zone. Based on Table 1, the inhibition zones of varying ZnO NPs concentrations against each bacteria strain were considerably different ($p< 0.001$). The Kruskal-Wallis assessment also indicated notable inhibition zone diameter variations between each ZnO NPs concentration, recording $H (6)= 56.898$ and $p< 0.001$. At lower concentrations (50–100 ug/mL), *B. subtilis* exhibited resistance against the ZnO NPs, while *E. coli* and *K. pneumoniae* were susceptible to the NPs at higher concentrations. Wider inhibition zones were observed with increasing ZnO NPs concentration. Nonetheless, the bacteria were the most susceptible against 250 µg/mL of ZnO NPs, documenting 3.3 ± 0.6 (*B. subtilis*), 5.9 ± 0.4 (*S. aureus*), 8.3 ± 0.3 (*K. pneumoniae*), and 8.3 ± 0.6 (*E. coli*) mm inhibition zones. The findings suggested a dose-dependent inhibitory effect of the ZnO NPs relative to their concentration. A positive correlation between inhibition zone diameter for each strain and NPs concentration was also noted by Karthik, M. *et al*. [31], Kamarajan, J. *et al*. [32], and Alamdari, S. *et al*. [14] (Figure S2).

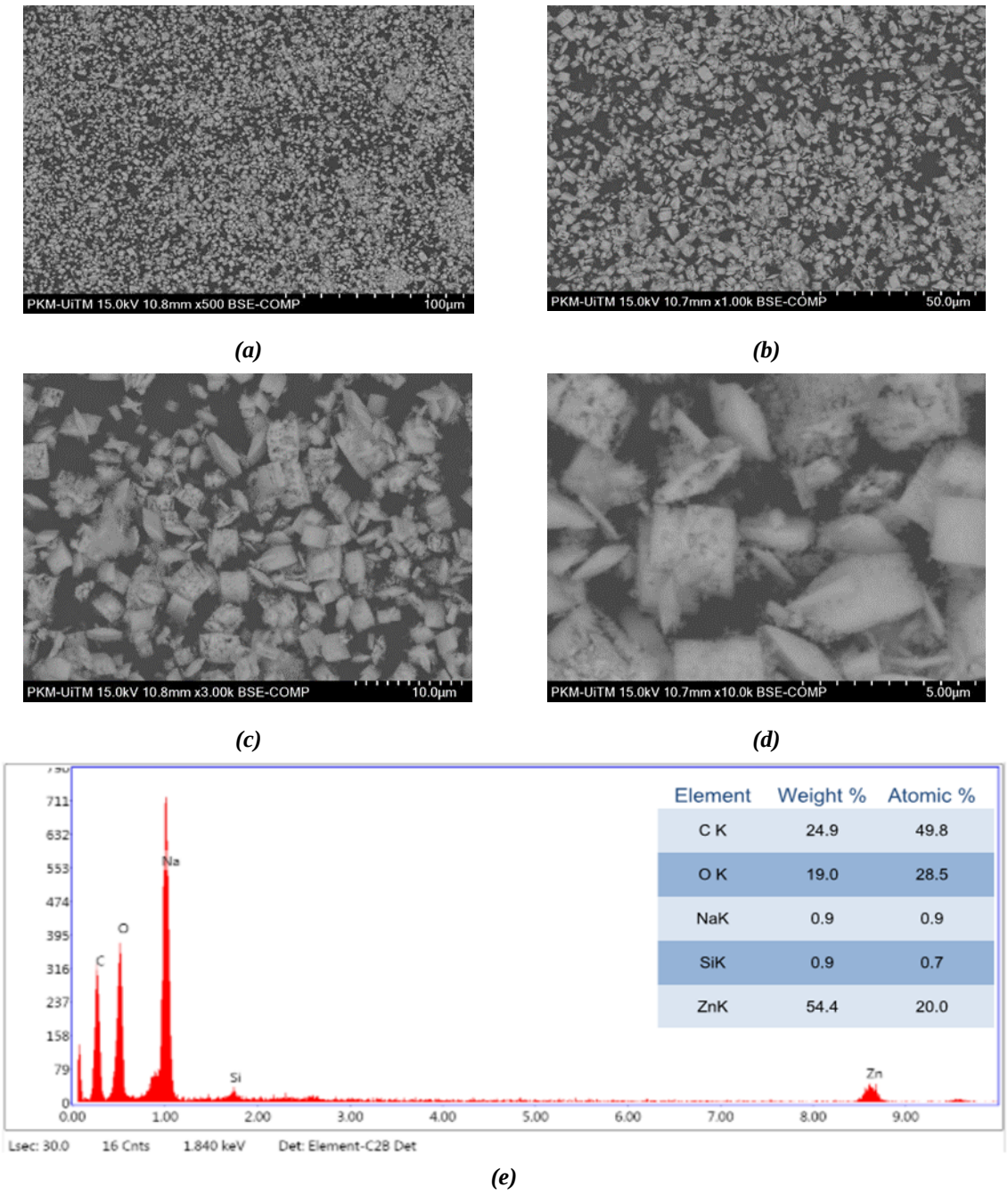

Figure 5. SEM of ZnO NPs at 100 µm *(a)*, 50 µm *(b)*, 10 µm *(c)*, 5 µm *(d)* and EDX analysis *(e)*.

Table 1

The inhibition zones of each bacterial strain assessed.

Bacteria	*Inhibition zone diameter (mm)*					*Positive control (10 µg of Ciprofloxacin)*	*Negative control (10 µg of distilled water)*
	ZnO NPs concentration						
	50 µg/mL	*100 µg/mL*	*150 µg/mL*	*200 µg/mL*	*250 µg/mL*		
B. subtilis	-	-	0.3 ± 0.6^{b}	2.8 ± 0.8^{c}	3.3 ± 0.6^{d}	25.7 ± 0.6^{a}	-
S. aureus	0.3 ± 0.6^{a}	3.8 ± 0.6^{b}	4.2 ± 0.7^{b}	5.2 ± 0.8^{b}	5.9 ± 0.4^{c}	28.3 ± 1.5^{b}	-
E. coli	3.8 ± 0.3^{a}	6.0 ± 0.8^{a}	7.2 ± 0.8^{a}	7.4 ± 0.5^{a}	8.3 ± 0.6^{a}	27.0 ± 1.0^{a}	-
K. pneumoniae	4.8 ± 0.3^{a}	5.4 ± 0.7^{a}	5.8 ± 0.3^{b}	7.4 ± 0.5^{c}	8.3 ± 0.3^{d}	28.3 ± 1.5^{a}	-
Kruskal Wallis df	2	2	3	3	3	3	
P	0.001	0.001	0.003	0.003	0.017	0.013	-

Note: - indicates no inhibition zone, the values are presented in mean ± SD, and the values with superscript letters are significantly different at (p< 0.01) within the column.

Table 2

The Spearman's Rho correlations between ZnO NPs concentration, inhibition zone diameter, and bacteria determined with SPSS.

	Concentration (µg/mL)	*Inhibition zone (mm)*	*Bacteria*
Concentration	1	0.063	0.000
Inhibition zone	0.063	1	0.425**
Bacteria	0.000	0.425**	1

(* sig p< 0.05 ** sig< 0.01)

Statistical analysis with Spearman's Rho indicated a significant correlation between inhibition zone diameters (0.063) and the bacteria evaluated (r= 0.425). The positive association implied that with rising ZnO NPs concentration, the bacterial inhibition zone diameter also improves (Table 2).

Conclusions

This study introduced a straightforward, cost-effective, and environmentally friendly approach to synthesising ZnO NPs employing *Oryza sativa* rice husks. The findings suggested that *Oryza sativa* RH could serve as an efficient reducing and capping agent for biosynthesis of ZnO NPs. The ZnO NPs procured in the present study were characterised with UV-Vis, XRD, TEM, FTIR, and SEM-EDX. The NPs were less than 21 nm, which was determined through the Debye–Scherrer's equation. The SEM-EDX analysis revealed the irregular and quadrilateral crystalline nature of the ZnO NPs, while the TEM results indicated its rod and worm-like shapes. The antibacterial efficacy of the biosynthesised ZnO NPs against Gram-negative (*E. coli* and *K. pneumoniae*) and Gram-positive (*S. aureus* and B. *subtilis*) bacteria was also established. The findings demonstrated the potential antibacterial treatment applications of the ZnO NPs due to their inherent toxicity, which could effectively inhibit bacterial growth by generating intracellular reactive oxygen species.

Acknowledgements

The authors would like to express gratitude to the Ministry of Higher Education for funding the present study through the Fundamental Research Grant Scheme (Grant No. FRGS-RMC 600 5/3 056/2022). The authors would also like to thank Universiti Teknologi MARA, Universiti Putra Malaysia, and Malaysian Agricultural Research and Development Institute (MARDI) for providing the facilities and plant materials for this study.

Supplementary information

Supplementary data are available free of charge at http://cjm.ichem.md as PDF file.

References

1. Demissie, M.G.; Sabir, F.K.; Edossa, G.D.; Gonfa, B.A. Synthesis of zinc oxide nanoparticles using leaf extract of *Lippia adoensis* (Koseret) and evaluation of its antibacterial activity. Journal of Chemistry, 2020, 7459042, pp. 1–9. DOI: https://doi.org/10.1155/2020/7459042
2. Hossain, N.; Islam, M.A.; Chowdhury, M.A. Synthesis and characterization of plant extracted silver nanoparticles and advances in dental implant applications. Heliyon, 2022, 8(12), e12313, pp. 1–13. DOI: https://doi.org/10.1016/j.heliyon.2022.e12313
3. Haddada, B.M.; Gerometta, E.; Chawech, R.; Sorres, J.; Bialecki, A.; Pesnel, S.; Spadavecchia, J.; Morel, A.-L. Assessment of antioxidant and dermoprotective activities of gold nanoparticles as safe cosmetic ingredient. Colloids and Surfaces B, 2020, 189, 110855, pp. 1–10. DOI: https://doi.org/10.1016/j.colsurfb.2020.110855
4. Singh, K.; Singh, J.; Rawat, M. Green synthesis of zinc oxide nanoparticles using *Punica Granatum* leaf extract and its application towards photocatalytic degradation of Coomassie brilliant blue R-250 dye. SN Applied Sciences, 2019, 1, 624, pp. 1–8. DOI: https://doi.org/10.1007/s42452-019-0610-5
5. Balogun, S.W.; James, O.O.; Sanusi, Y.K.; Olayinka, O.H. Green synthesis and characterization of zinc oxide nanoparticles using bashful (*Mimosa pudic*a), leaf extract: a precursor for organic electronics applications. SN Applied Sciences, 2020, 2, 504, pp. 1–8. DOI: https://doi.org/10.1007/s42452-020-2127-3
6. Sedefoglu, N.; Zalaoglu, Y.; Bozok, F. Green synthesized ZnO nanoparticles using *Ganoderma lucidum*: Characterization and *In Vitro* Nanofertilizer effects. Journal of Alloys and Compounds, 2022, 918, 165695, pp. 1–8. DOI: https://doi.org/10.1016/j.jallcom.2022.165695
7. Al-Khafaji, M.A.A.; Al-Refai'a, R.A.K.; Al-Zamely, O.M.Y. Green synthesis of copper nanoparticles using artemisia plant extract. Materials Today: Proceedings, 2022, 49(7), pp. 2831–2835. DOI: https://doi.org/10.1016/j.matpr.2021.10.067
8. Moreno-Luna, F.B.; Herrera-Pérez, J.L.; Bautista-Hernández, A.; Meraz-Melo, M.A.; Santoyo-Salazar, J.; Vázquez-Cuchillo, O. Biosynthesis of gold nanoparticles from *Agave potatorum* extracts: effect of the solvent in the

extraction. Materials Today Sustainability, 2022, 20, 100231, pp. 1–8.
DOI: https://doi.org/10.1016/j.mtsust.2022.100231
9. Singh, R.; Hano, C.; Nath, G.; Sharma, B. Green biosynthesis of silver nanoparticles using leaf extract of *Carissa carandas L.* and their antioxidant and antimicrobial activity against human pathogenic bacteria. Biomolecules, 2021, 11(2), 299, pp. 1–10.
DOI: https://doi.org/10.3390/biom11020299
10. Abdelbaky, A.S.; Abd El-Mageed, T.A.; Babalghith, A.O.; Selim, S.; Mohamed, A.M.H.A. Green synthesis and characterization of ZnO nanoparticles using *Pelargonium odoratissimum* (L.) aqueous leaf extract and their antioxidant, antibacterial and anti-inflammatory activities. Antioxidants, 2022, 11(8), 1444, pp. 1–25.
DOI: https://doi.org/10.3390/antiox11081444
11. El-Belely, E.F.; Farag, M.M.S.; Said, H.A.; Amin, A.S.; Azab, E.; Gobouri, A.A.; Fouda, A. Green synthesis of zinc oxide nanoparticles (ZnO-NPs) using *Arthrospira platensis* (class: Cyanophyceae) and evaluation of their biomedical activities. Nanomaterials, 2021, 11(1), 95, pp. 1–18.
DOI: https://doi.org/10.3390/nano11010095
12. Al-Naamani, L.; Dobretsov, S.; Dutta, J. Chitosan-zinc oxide nanoparticle composite coating for active food packaging applications. Innovative Food Science & Emerging Technologies, 2016, 38(A), pp. 231–237.
DOI: https://doi.org/10.1016/j.ifset.2016.10.010
13. Sankapal, B.R.; Gajare, H.B.; Karade, S.S.; Salunkhe, R.R.; Dubal, D.P. Zinc oxide encapsulated carbon nanotube thin films for energy storage applications. Electrochim Acta, 2016, 192, pp. 377–384.
DOI: https://doi.org/10.1016/j.electacta.2016.01.193
14. Alamdari, S.; Ghamsari, M.S.; Lee, C.; Han, W.; Park, H.H.; Tafreshi, M.J.; Afarideh, H.; Ara, M.H.M. Preparation and characterization of zinc oxide nanoparticles using leaf extract of *Sambucus ebulus*. Applied Sciences, 2020, 10(10), 3620, pp. 1–19.
DOI: https://doi.org/10.3390/app10103620
15. Abdolhoseinzadeh, A.; Sheibani, S. Enhanced photocatalytic performance of Cu_2O nano-photocatalyst powder modified by ball milling and ZnO. Advanced Powder Technology, 2020, 31(1), pp. 40–50.
DOI: https://doi.org/10.1016/j.apt.2019.09.035
16. Hernández, R.; Hernández-Reséndiz, J.R.; Martínez-Chávez, A.; Velázquez-Castillo, R.; Escobar-Alarcón, L.; Esquivel, K. X-ray diffraction Rietveld structural analysis of Au–TiO_2 powders synthesized by sol–gel route coupled to microwave and sonochemistry. Journal of Sol-Gel Science and Technology, 2020, 95, pp. 239–252.
DOI: https://doi.org/10.1007/s10971-020-05264-5
17. Kolodziejczak-Radzimska, A.; Jesionowski, T. Zinc oxide-from synthesis to application: A review. Materials, 2014, 7(4), pp. 2833–2881.
DOI: https://doi.org/10.3390/ma7042833
18. Al Awadh, A.A.; Shet, A.R.; Patil, L.R.; Shaikh, I.A.; Alshahran,i M.M.; Nadaf, R.; Mahnashi, M.H.; Desai, S.V.; Muddapur, U.M.; Achappa, S.; Hombalimath, V.S.; Khan, A.A.; Gouse, H.S.M.; Iqubal, S.M.S.; Kumbar, V. Sustainable synthesis and characterization of zinc oxide nanoparticles using *Raphanus sativus* extract and its biomedical applications. Crystals, 2022, 12(8), 1142, pp. 1–18.
DOI: https://doi.org/10.3390/cryst12081142
19. Velsankar, K.; Venkatesan, A.; Muthumari, P.; Suganya, S,; Mohandoss, S.; Sudhahar, S. Green inspired synthesis of ZnO nanoparticles and its characterizations with biofilm, antioxidant, anti-inflammatory, and anti-diabetic activities. Journal of Molecular Structure, 2022, 1255, 132420, pp. 1–15. DOI: https://doi.org/10.1016/j.molstruc.2022.132420
20. Brishti, R.S.; Habib, A.M.; Ara, M.H.; Rezaul Karim, K.M.; Khairul Islam, M.; Naime, J.; Hasan Rumon, M.M.; Khan, M.A.R. Green synthesis of ZnO NPs using aqueous extract of *Epipremnum aureum* leave: Photocatalytic degradation of Congo red. Results in Chemistry, 2024, 7, 101441, pp. 1–11.
DOI: https://doi.org/10.1016/j.rechem.2024.101441
21. Hussain, A.; Oves, M.; Alajmi, M.F.; Hussain, I.; Amir, S.; Ahmed, J.; Rehman, M.T.; El-Seedi, H.R.; Ali, I. Biogenesis of ZnO nanoparticles using *Pandanus odorifer* leaf extract: anticancer and antimicrobial activities. RSC Advances, 2019, 9(27), pp. 15357–15369.
DOI: https://doi.org/10.1039/c9ra01659g
22. Saka, A.; Tesfaye, J.L.; Nagaprasad, N.; Shanmugam, R.; Dwarampudi, L.P.; Krishnaraj, R. Synthesis and characterization of zinc oxide nanoparticles using *Moringa* leaf extract. Journal of Nanomaterials, 2021, 4525770, pp. 1–6.
DOI: https://doi.org/10.1155/2021/4525770
23. Saka, A.; Tesfaye, J.L.; Gudata, L.; Shanmugam, R.; Dwarampudi, L.P.; Nagaprasad, N.; Krishnaraj, R.; Rajeshkumar, S. Synthesis, characterization, and antibacterial activity of ZnO nanoparticles from fresh leaf extracts of Apocynaceae, *Carissa spinarum* L. (Hagamsa). Journal of Nanomaterials, 2022, 6230298, pp. 1–6.
DOI: https://doi.org/10.1155/2022/6230298
24. Jan, H.; Shah, M.; Andleeb, A.; Faisal, S.; Khattak, A.; Rizwan, M.; Drouet, S.; Hano, C.; Abbasi, B.H. Plant-based synthesis of zinc oxide nanoparticles (ZnO-NPs) using aqueous leaf extract of *Aquilegia pubiflora*: their antiproliferative activity against HepG2 Cells Inducing Reactive Oxygen Species and other *in vitro* properties. Oxidative Medicine and Cellular Longevity, 2021, 4786227, pp. 1–14.
DOI: https://doi.org/10.1155/2021/4786227
25. Supiyani, S.; Agusnar, H.; Sugita, P.; Nainggolan, I. Preparation sodium silicate from rice husk to synthesize silica nanoparticles by sol-gel method for adsorption water in analysis of methamphetamine. South African Journal of Chemical Engineering, 2022, 40, pp. 80–86.

DOI: https://doi.org/10.1016/j.sajce.2022.02.001
26. Mezan, S.O.; Al Absi, S.M.; Jabbar, A.H.; Roslan, M.S.; Agam, M.A. Synthesis and characterization of enhanced silica nanoparticle (SiO_2) prepared from rice husk ash immobilized of 3-(chloropropyl) triethoxysilanea. Materials Today: Proceedings, 2021, 42(5), pp. 2464–2468. DOI: https://doi.org/10.1016/j.matpr.2020.12.564
27. Azat, S.; Korobeinyk, A.V.; Moustakas, K.; Inglezakis, V.J. Sustainable production of pure silica from rice husk waste in Kazakhstan. Journal of Cleaner Production, 2019, 217, pp. 352–359. DOI: https://doi.org/10.1016/j.jclepro.2019.01.142
28. Nguyen, H.X.; Dao, N.T.T.; Nguyen, H.T.T.; Le, A.Q.T. Nanosilica synthesis from rice husk and application for soaking seeds. IOP Conference Series: Earth and Environmental Science, 2019, 266, 012007, pp. 1–10. DOI: https://doi.org/10.1088/1755-1315/266/1/012007
29. Rahman, R.A.; Hua, C.C.; Masdor, N.A. Green synthesis and characterization of zinc oxide nanoparticles using *Aloe Vera* leaf extract. AIP Conference Proceedings, 2023, 2703(1), 120006, pp. 1–8. DOI: https://doi.org/10.1063/5.0115328
30. Ali, D.; Arooj, N.; Muneer, I.; Bashir, F.; Hanif, M.; Ali, S. Sustainable synthesis of ZnO nanoparticles from *Psathyrella candolleana* mushroom extract: Characterization, antibacterial activity, and photocatalytic potential. Inorganic Chemistry Communications, 2023, 158(2), 111588, pp. 1–13. DOI: https://doi.org/10.1016/j.inoche.2023.111588
31. Karthik, M.; Ragunath, C.; Krishnasamy, P.; Paulraj, D.; Ramasubramanian, V. Green synthesis of zinc oxide nanoparticles using *Annona muricata* leaf extract and its antioxidant and antibacterial activity. Inorganic Chemistry Communications, 2023, 157, 111422, pp. 1–9. DOI: https://doi.org/10.1016/j.inoche.2023.111422
32. Kamarajan, D.; Anburaj, B.; Porkalai, V.; Muthuvel, A.; Nedunchezhian, G.; Mahendran, N. Green synthesis of ZnO nanoparticles and their photocatalyst degradation and antibacterial activity. Journal of Water and Environmental Nanotechnology, 2022, 7(2), pp. 180–193. DOI: https://doi.org/10.22090/jwent.2022.02.006
33. Sakthivel, S.; Dhanapal, A.R.; Paulraj, L.P.; Gurusamy, A.; Venkidasamy, B.; Thiruvengadam, M.; Govindasamy, R.; Shariati, M.A.; Bouyahya, A.; Zengin, G.; Hasan, M.M.; Burkov, P. Antibacterial activity of seed aqueous extract of *Citrus limon* (L.) mediated synthesis ZnO NPs: An impact on Zebrafish (*Danio rerio*) caudal fin development. Heliyon, 2022, 8(9), e10406, pp. 1–9. DOI: https://doi.org/10.1016/j.heliyon.2022.e10406
34. Iqbal. J.; Abbasi, B.A.; Yaseen, T.; Zahra, S.A.; Shahbaz, A.; Shah, S.A.; Uddin, S.; Ma, X.; Raouf, B.; Kanwal, S.; Amin, W.; Mahmood, T.; HamedA. El-Serehy, H.A.; Ahmad, P. Green synthesis of zinc oxide nanoparticles using *Elaeagnus angustifolia* L. leaf extracts and their multiple in vitro biological applications. Scientific Reports, 2021, 11, 20988, pp. 1–13. DOI: https://doi.org/10.1038/s41598-021-99839-z
35. Sundrarajan, M.; Ambika, S.; Bharathi, K. Plant-extract mediated synthesis of ZnO nanoparticles using *Pongamia pinnata* and their activity against pathogenic bacteria. Advanced Powder Technology, 2015, 26(5), pp. 1294–1299. DOI: https://doi.org/10.1016/j.apt.2015.07.001
36. Jayappa, M.D.; Ramaiah, C.K.; Kumar, M.A.P.; Suresh, D.; Prabhu, A.; Punchappady-Devasya, R.; Sheikh, S. Green synthesis of zinc oxide nanoparticles from the leaf, stem and in vitro grown callus of *Mussaenda frondosa* L.: characterization and their applications. Applied Nanoscience, 2020, 10, pp. 3057–3074. DOI: https://doi.org/10.1007/s13204-020-01382-2
37. Ansari, A,; Ali, A,; Khan, N.; Saad Umar, M.; Owais, M.; Shamsuzzaman Synthesis of steroidal dihydropyrazole derivatives using green ZnO NPs and evaluation of their anticancer and antioxidant activity. Steroids, 2022, 188, 109113, pp. 1–14. DOI: https://doi.org/10.1016/j.steroids.2022.109113
38. Gangwar, J.; Balasubramanian, B.; Pratap Singh, A.; Meyyazhagan, A.; Pappuswamy, M.; Alanazi, A.M.; Rengasamy, K.R.R.; Joseph, K.S. Biosynthesis of zinc oxide nanoparticles mediated by *Strobilanthes hamiltoniana*: Characterizations, and its biological applications. Kuwait Journal of Science, 2024, 51(1), 100102, pp. 1–9. DOI: https://doi.org/10.1016/j.kjs.2023.07.008
39. Gayathri Devi, K.; Clara Dhanemozhi, A.; Sathya Priya, L. Green synthesis of Zinc oxide nanoparticles using lemon extract for waste water treatment. Materials Today: Proceedings, 2023, pp. 1–8. DOI: https://doi.org/10.1016/j.matpr.2023.03.576
40. Suhel, A.; Abdul Rahim, N.; Abdul Rahman, M.R.; Bin Ahmad, K.A.; Khan, U.; Teoh, Y.H.; Abidin, N.Z. Impact of ZnO nanoparticles as additive on performance and emission characteristics of a diesel engine fueled with waste plastic oil. Heliyon, 2023, 9(4), e14782, pp. 1–16. DOI: https://doi.org/10.1016/j.heliyon.2023.e14782
41. Shaghaghi, Z,; Mollaei, S.; Amani-Ghadim, A.R.; Abedini, Z. Green synthesis of ZnO nanoparticles using the aqueous extract of *Platanus orientalis*: Structural characterization and photocatalytic activity. Materials Chemistry and Physics, 2023, 305, 127900, pp. 1–37. DOI: https://doi.org/10.1016/j.matchemphys.2023.127900
42. Selçuk Pekdemir, S.; Bakar, B.; Tas, R.; Ulu, A.; Pekdemir, M.E.; Ateş, B. Immobilization of Xylanase on ZnO nanoparticles obtained by green synthesis from *Eupatorium cannabinum* L. and its application in enrichment of fruit juices. Molecular Catalysis, 2024, 562, 114232, pp. 1–11. DOI: https://doi.org/10.1016/j.mcat.2024.114232